SPANDIDOS PUBLICATIONS

ONCOLOGY LETTERS 14: 6678-6684, 2017

Ouabain targets the Na^+/K^+-ATPase α_3 isoform to inhibit cancer cell proliferation and induce apoptosis

YIJUN XIAO, CHEN MENG, JIE LIN, CHAOQUN HUANG, XIULI ZHANG, YANYU LONG, YIDE HUANG and YAO LIN

College of Life Sciences, Fujian Normal University, Fuzhou, Fujian 350117, P.R. China

Received July 1, 2016; Accepted July 14, 2017

DOI: 10.3892/ol.2017.7070

Abstract. Ouabain has been used for the treatment of heart failure and atrial fibrillation. Its potential anticancer effect has also attracted great interest. The aim of the present study was to evaluate the anticancer effect of ouabain and investigate its molecular target. The effects of ouabain on the viability of and induction of cellular death on OS-RC-2 renal cancer cells were examined using the MTT assay and acridine orange/ethidium bromide staining. The levels of Ca^{2+} and reactive oxygen species were determined using Fura-3-acetoxymethyl ester and dichloro-dihydro-fluorescein diacetate probes, respectively. Apoptosis was examined using annexin V-fluorescein isothiocyanate/propidium iodide staining and western blotting. The expression profile of the different Na^+/K^+-ATPase (NKA) isoforms in NCI-H446 small cell lung cancer cells was determined using immunocytochemistry and reverse transcription polymerase chain reaction analysis. In the present study, it was demonstrated that ouabain inhibited cancer cell proliferation and induced apoptosis while no significant difference in the expression of NKA α_1 and α_3 isoforms was detected following 48 h of ouabain treatment. Furthermore, expression of NKA α_3 but not the α_1 isoform was associated with ouabain sensitivity. The results of the present study indicated that ouabain targets the NKA α_3 isoform, inhibits cancer cell proliferation and induces apoptosis.

Correspondence to: Professor Yao Lin, College of Life Sciences, Fujian Normal University, Qishan Campus, 1 Keji Road, Fuzhou, Fujian 350117, P.R. China
E-mail: yaolin@fjnu.edu.cn

Abbreviations: NKA, Na^+/K^+-ATPase; ICC, immunocytochemistry; ROS, reactive oxygen species; IC_{50}, half-maximal inhibitory concentration; AO/EB, acridine orange/ethidium bromide; DCFH-DA, dichloro-dihydro-fluorescein diacetate; Bcl-2, B-cell lymphoma 2; Bax, Bcl-2-associated X protein; RT, room temperature; siRNA, small interfering RNA

Key words: ouabain, proliferation, apoptosis, Na^+/K^+-ATPase

Introduction

Cancer refers to a group of diseases resulting from uncontrolled cellular growth. It is a major concern for public healthcare, and data from GLOBOCAN revealed that ~14.1 million new cancer cases and 8.2 million cancer-associated mortality occurred worldwide in 2012 (1).

Na^+/K^+-ATPase (NKA), which functions as a sodium-potassium pump, is a ubiquitous enzyme that serves as an ion transporter and a signal transducer (2). This enzyme consists of one α and one β subunit (2). The NKA pumps two K^+ into cells and three Na^+ out of cells using energy derived from ATP (2). NKA serves a critical function in cellular growth, differentiation and survival as well as cell migration and cell-cell interaction (2). Since 1957, when Jens Christian Skou discovered NKAs, increasing evidence suggests that NKAs not only maintain cell membrane potential, but also serve an important function in cancer (3-5). Alterations in NKA expression and function have been documented in several types of cancer including colorectal cancer and liver metastases (3). It has been reported that the α_1 and α_3 NKA isoforms are overexpressed in tumor cells and metastases, including hepatocellular carcinoma (5).

Ouabain is a highly specific inhibitor of NKA and has been used for the treatment of heart failure and atrial fibrillation (6). There has been renewed interest in the anticancer effect of ouabain as epidemiological studies have revealed that administration of ouabain in patients with cancer significantly improved survival rates (7-12). A study by Xu *et al* (13) demonstrated that ouabain binds to the NKA signalosome and activates multiple signaling pathways associated with cell death and apoptosis. However, the molecular mechanisms underlying the anticancer effect of ouabain remain unclear. The results of the present study revealed that the anticancer effect of ouabain is associated with inhibition of the NKA α_3 isoform rather than the α_1 isoform.

Materials and methods

Cell culture. The human renal cancer cell line OS-RC-2 was purchased from the Type Culture Collection of the Chinese Academy of Sciences (Shanghai, China). The human small cell lung cancer cell line NCI-H446 was obtained from the Fujian Institute of Hematology (Fuzhou, China). These cell lines were

maintained at 37˚C in RPMI-1640 medium (Gibco; Thermo Fisher Scientific, Inc., Waltham, MA, USA) supplemented with 10% fetal bovine serum (Equitech-Bio, Inc., Kerrville, TX, USA) and 1% penicillin G and streptomycin (Invitrogen; Thermo Fisher Scientific, Inc.). Ouabain was purchased from Sigma-Aldrich; Merck KGaA (Darmstadt, Germany). All cells were maintained in 5% CO_2 at 37˚C.

MTT assay. Cells were seeded in 96-well plates (3,000 cells/well with 180 μl RPMI-1640) and treated with either DMSO or ouabain (20, 40, 80, 160, 320 nM). Subsequently, cells were incubated for the indicated period of time (24, 48 and 72 h), cell viability was determined using the MTT assay kit (Roche Diagnostics GmbH, Mannheim, Germany), according to the manufacturer's protocol. The quantity of formazan was determined by recording changes in absorbance at 490 nm. Each assay was performed in triplicate. Comparisons were performed using one-way analysis of variance (ANOVA).

Acridine orange/ethidium bromide (AO/EB) staining. Cells were seeded in 6-well plates at a density of $1x10^5$ cells per well. Cells were treated with ouabain (0, 20, 40, 80 nM) and incubated in 5% CO_2 at 37˚C for 48 h and stained with the AO/EB dye solution containing 200 μg/ml AO (Sigma-Aldrich; Merck KGaA) and 200 μg/ml EB (Sino-American Biotechnology Co., Luoyang, China) at room temperature for 1 min. Cells were then immediately observed using a fluorescence inverted microscope (magnification, x400; BX51-P; Olympus Corporation, Tokyo, Japan) and 10 fields of views were assessed.

AnnexinV-fluorescein isothiocyanate (FITC)/propidium iodide (PI) flow cytometric analysis. Cells were seeded in 6-well plates at a density of $2x10^5$ cells per well. 24 h later, cells were treated with ouabain at 37˚C for 48 h and then flow cytometric analysis was performed to assess cellular apoptosis using the AnnexinV-FITC/PI Apoptosis Detection kit (Beyotime Institute of Biotechnology, Haimen, China) according to the manufacturer's protocol. Apoptotic cells were analyzed using a flow cytometer and FlowJo software (version 10; FlowJo LLC, Ashland, OR, USA).

Ca^{2+} and reactive oxygen species (ROS) quantification. Cells were treated at 37˚C with ouabain for 48 h and then washed with PBS. The fluorescence probes Fura-3-acetoxymethyl ester (AM) and dichloro-dihydro-fluorescein diacetate (DCFH-DA; Beyotime Institute of Biotechnology) were used at concentrations of 10 and 2 μM, respectively. Cells were then incubated in RPMI-1640 medium containing the fluorescence probes in the dark for 20-40 min at 37˚C and washed for 30 min in serum-free RPMI-1640 medium. Fluorescence images were captured using a confocal microscope (magnification, x400; C1SI; Nikon Corporation, Tokyo, Japan). The excitation wavelength was 488 nm and the emission wavelength was 522-530 nm. The fluorescence intensity was assessed using Image-Pro Plus software6.0 (Media Cybernetics, Inc., Rockville, MD, USA).

Isolation of apoptotic DNA fragments. Cells treated at 37˚C with different concentrations (0, 10, 20, 40 nM) of ouabain for 48 h, cells were collected and treated for 10 sec with lysis buffer (50 mM Tris-Cl, 150 mM NaCl, 1% nonylphenoxypolyethoxyl ethanol, 1% sodium deoxycholate and 1% SDS) at room temperature (RT). Supernatant was collected by centrifugation for 5 min at 14,000 x g, 1% SDS was added and samples were then treated with ribonuclease A for 2 h at 56˚C followed by digestion with proteinase K for at least 2 h at 37˚C. Subsequently, 0.5 volume 10 M ammonium acetate was added, the DNA was precipitated with 2.5 volume ethanol, dissolved in gel loading buffer (Sigma-Aldrich; Merck KGaA) and separated by electrophoresis on 1% agarose gels.

Western blotting. Total protein was extracted from cells using radio immunoprecipitation assay buffer (Beyotime Institute of Biotechnology) supplemented with protease inhibitors (Roche Diagnostics, Basel, Switzerland) at 4˚C for 30 min, and western blot analysis was performed as described previously (12). Primary antibodies against B-cell lymphoma 2 (Bcl-2; cat. no. 12789-1-AP; 1:2,000; Protein Tech Group, Inc., Chicago, IL, USA), Bcl-2-associated X protein (Bax; cat. no. BM3964; 1:500; Boster Biological Technology, Pleasanton, CA, USA) and β-actin (cat. no. 4967S; 1:2,000; Cell Signaling Technology, Inc., Danvers, MA, USA) were incubated with the membranes overnight at 4˚C. Following the primary incubation, membranes were incubated with horseradish peroxidase-conjugated goat anti-rabbit IgG or anti-mouse IgG secondary antibodies (Sigma-Aldrich; Merck KGaA).

Immunocytochemistry (ICC). Cells were seeded on coverslips at a density of $1x10^5$ cells. 24 h later cells were fixed with 0.4% paraformaldehyde at room temperature for 20 min and endogenous peroxidase activity was blocked with hydrogen peroxide for 30 min. To prevent non-specific binding cells were blocked with fetal bovine serum at room temperature for 30 min prior to primary antibody (Na/K-ATPase α1 antibody; cat. no. sc-58629, 1:1,000; Na/K-ATPase α3 antibody; cat. no. sc-71640; 1:1,000; Santa Cruz Biotechnology, Inc., Dallas, TX, USA) incubation overnight at 4˚C in a moist chamber. Cells were subsequently incubated with secondary antibodies (horseradish peroxidase-conjugated goat anti-mouse immunoglobulin G; cat. no, sc-2031; 1:2,000; Santa Cruz Biotechnology, Inc.) for 30 min at 37˚C and stained with 3,3'-diaminobenzidine for 5 min at RT. Cell nuclei were counterstained with hematoxylin at room temperature for 3 min and cells were finally dehydrated and mounted. Cells were visualized using a fluorescence inverted microscope (magnification, x400; BX51-P; Olympus Corporation, Tokyo, Japan) and 10 fields of views were assessed using Image-Pro Plus software 6.0 (Media Cybernetics, Inc.).

Reverse transcription polymerase chain reaction. Total RNA was extracted using TRIzol® reagent (Takara Bio, Inc., Otsu, Japan), according to the manufacturer's protocol. Total RNA was reverse transcribed into cDNA using the Reverse Transcription System (Takara Bio, Inc.). Subsequently, RT-qPCR was performed using miScript SYBR® green PCR Kit (Qiagen GmbH, Hilden, Germany), according to the manufacturer's protocol using specific primers for NKA isoform α_1, NKA α_3 and β-actin. The PCR conditions were as follows: 95˚C for 30 sec and then 40 cycles of 95˚C for 5 sec and 60˚C

for 34 sec. The expression levels of genes were determined using the $^{\Delta\Delta}$Cq method (14). The following primer pairs were used: β-actin forward: 5'-AACACCCCAGCCATGTACG-3' and reverse, 5'-ATGTCACGCACGATTTCCC-3'; NKA isoform α_1 forward, 5'-TGTCCAGAATTGCAGGTCTTTG-3' and reverse, 5'-TGCCCGCTTAAGAATAGGTAGGT-3' and NKA isoform α_3 forward, 5'-AAGGAGGTGGCTATGACA GAG-3' and reverse, 5'-GTGAGTGCGTTAGGCCCAT-3'.

Small interfering (si)RNA transfection. siRNA transfection was performed using Lipofectamine 2000 (Invitrogen; Thermo Fisher Scientific, Inc.), according to the manufacturer's guidelines. The control scramble siRNA (sc-37007), Na^+/K^+-ATPase α1 siRNA (sc-36010) and Na^+/K^+-ATPase α3 siRNA (sc-149790) were purchased from Santa Cruz Biotechnology, Inc. (Dallas, TX, USA).

Statistical analysis. Data were analyzed using Prism 5.0 software (Graphpad Software, Inc., La Jolla, CA, USA). Results are presented as the mean ± standard deviation of three independent experiments. Comparisons were performed by one-way analysis of variance followed by Dunnett's post hoc test. $P<0.05$ was considered to indicate a statistically significant difference.

Results

Ouabain inhibits proliferation of OS-RC-2 and NCI-H446 cells. To examine the effect of ouabain on cellular proliferation, OS-RC-2 cells were treated with different concentrations of ouabain (0, 20, 40, 80, 160, 320 nM) for 24, 48 and 72 h (Fig. 1A). Ouabain inhibited cancer cell proliferation in a time-dependent manner. The proportion of viable cells following ouabain treatment were measured using MTT assay. As the effect on cell proliferation was greater at 48 h in OS-RC-2 cells, this time point was selected for the experiments of this study, unless otherwise stated. The half-maximal inhibitory concentration n(IC_{50}) value of ouabainin OS-RC-2 cells, determined using the MTT assay, was ~39 nM (Fig. 1B). These results indicated that ouabain inhibited proliferation of OS-RC-2 cells in a dose- and time-dependent manner. Similar experiments were performed in NCI-H446 cells generating similar results (Fig. 1B). This suggests that the anti-proliferative effect of ouabain may apply to other cancer cell lines.

Ouabain induces cell death in OS-RC-2 and NCI-H446 cells. To investigate the underlying molecular mechanism of cell death induced by ouabain, treated cells were observed under an inverted and a fluorescent microscope. Morphological changes were induced inOS-RC-2 (Fig. 2A) and NCI-H446 (Fig. 2B) cells treated with a range of ouabain concentrations for 48 h. Cells treated with different concentrations of ouabain presented typical cell death features including membrane blebbing, cell shrinkage, detachment, nuclear condensation and fragmentation. AO/EB staining was then performed to confirm cell death. Red-orange fluorescence was enhanced in OS-RC-2 (Fig. 2C) and NCI-H446 (Fig. 2D) cells treated with increasing concentrations of ouabain; indicating that ouabain induces cell death.

Ouabain increases the intracellular Ca^{2+} and ROS levels (15). Majno and Joris (16) reported that an increasing concentrations of intracellular Ca^{2+} and ROS serves a key function in cell death. Thus, to investigate whether ouabain caused changes in Ca^{2+} and ROS levels, OS-RC-2 and NCI-H446 cells were treated with a range of ouabain concentrations and the Ca^{2+} and ROS levels were examined using Fura-3-AM and DCFH-DA probes, respectively. OS-RC-2 (Fig. 2E and F) and NCI-H446 (Fig. 2G and H) cells treated with ouabain presented significantly higher Ca^{2+} and ROS fluorescence intensity compared with the untreated control group ($P<0.05$), suggesting that ouabain induces cell death.

Ouabain induces apoptosis. To investigate whether ouabain induces apoptosis, flow cytometric analysis with annexin V staining was performed. As presented in Fig. 3A and B, increasing concentration of ouabain significantly induced apoptosis ($P<0.01$). In addition, a key feature of apoptosis is DNA fragmentation, which it is possible to visualize as DNA laddering following separation by gel electrophoresis (17). OS-RC-2 and NCI-H446 cells were treated with a range of ouabain concentrations and DNA laddering was visualized following separation by gel electrophoresis (Fig. 3C and D). Apoptosis regulator Bax is a pro-apoptotic member of the Bcl-2 family, while other members including Bcl-2 inhibit apoptosis (17). As presented in Fig. 3E, OS-RC-2 cells treated with a range of ouabain concentrations for 48 h demonstrated a dose-dependent increase in Bax protein levels and a decrease in Bcl-2 protein levels. These results suggested that ouabain induces apoptosis in cancer cells.

The anticancer effect of ouabain was associated with think α_3 isoform rather than the α_1 isoform. To investigate the involvement of NKA in the anticancer effect of ouabain, the expression of the NKA α_1 and α_3 isoforms was determined using ICC staining in NCI-H446 cells treated with a range of ouabain concentrations (Fig. 4A and B). The expression levels of the NKA α_1 and α_3 isoformswere determined using Image-Pro Plus software 6.0 and no significant difference was observed between treated and untreated cells. These results indicated that ouabain had no effect on the expression of NKA α_1 and α_3 isoforms.

To further investigate the underlying molecular mechanism, transfection with siRNAs targeting the NKA α_1 and α_3 isoforms was performed in NCI-H446 cells. As presented in Fig. 5A and B, mRNA and protein expression of the NKA α_1 and α_3 isoforms was significantly decreased following siRNA transfection. NCI-H446 siRNA transfected cells were then treated with ouabain. As presented in Fig. 5C and D, only the siRNA targeting the NKA α_3 isoform antagonized the effect of ouabain; indicating that ouabain sensitivity is associated with the NKA α_3 isoform rather than α_1 isoform.

Discussion

Targeted therapy is expected to be more effective than conventional treatments and less toxic to normal cells. Several studies have demonstrated that NKA expression is associated with cancer mortality rates (3,5,18). Therefore, NKA has attracted a lot of interest as an anticancer target.

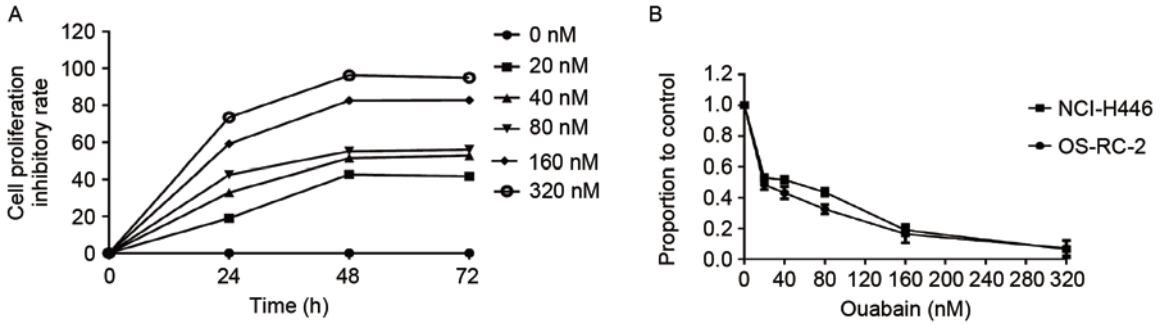

Figure 1. Ouabain inhibits cancer cell proliferation. (A) Ouabain inhibited the proliferation of OS-RC-2 cancer cells in a dose- and time-dependent manner. (B) Cells (NCI-H446 and OS-RC-2) were treated with different concentrations of ouabain (0, 20, 40, 80, 160, 320 nM) for 48 h and the half-maximal inhibitory concentration was determined using the MTT assay.

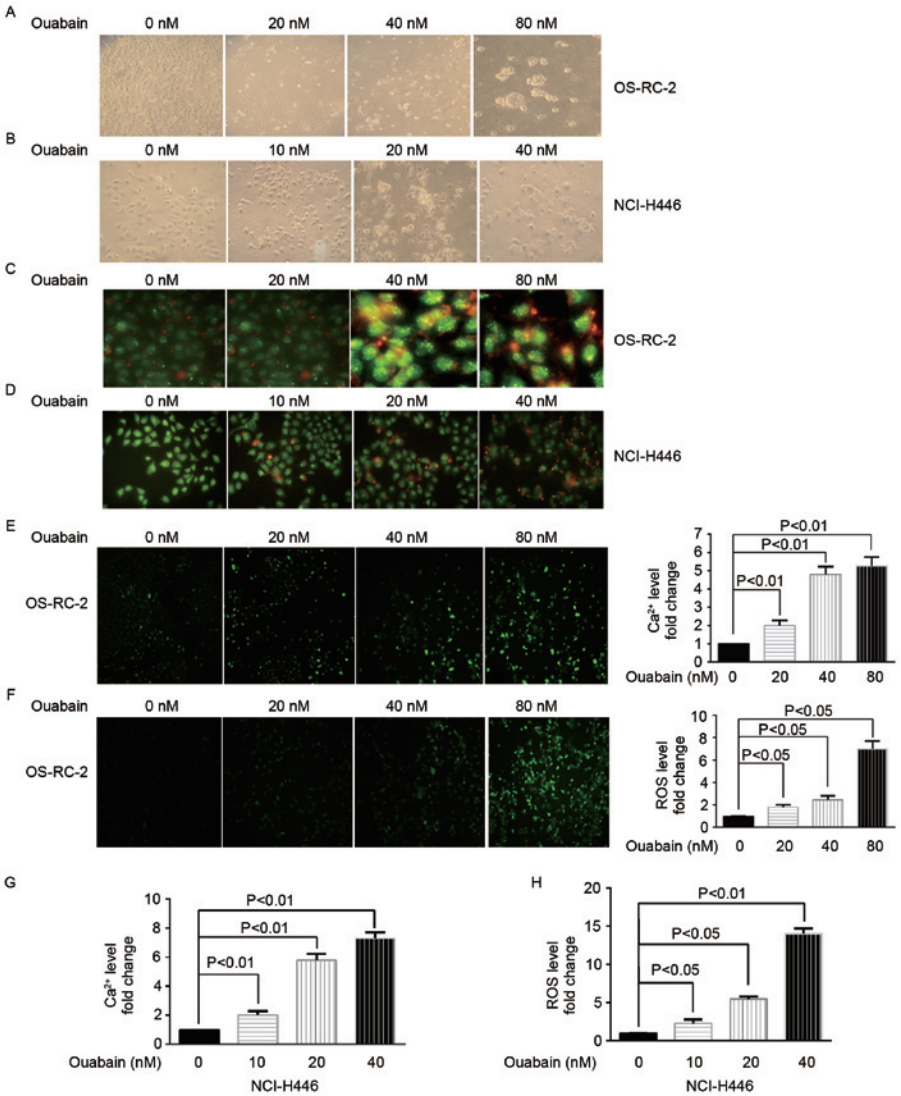

Figure 2. Ouabain induces cell death. (A) OS-RC-2 cells treated with a range of ouabain concentrations (0, 20, 40 and 80 nM) for 48 h were observed under an inverted microscope (magnification, x400). (B) NCI-H446 cells treated with a range of ouabain concentrations (0, 10, 20 and 40 nM) for 48 h were observed under an inverted microscope (magnification, x400). (C) OS-RC-2 cells treated with a range of ouabain concentrations (0, 20, 40 and 80 nM) for 48 h were stained with AO/EB dye solution and observed under a confocal microscope (magnification, x400). (D) NCI-H446 cells treated with a range of oubain concentrations (0, 10, 20 and 40 nM) for 48 h were stained with AO/EB dye solution and observed under a confocal microscope (magnification, x400). (E) Intracellular Ca^{2+} levels determined using a Fura-3/AM probe in OS-RC-2 cells treated with a range of ouabain concentrations (0, 20, 40 and 80 nM) for 48 h, using a confocal microscope (magnification, x400). (F) Intracellular ROS levels determined using a DCFH-DA probe in OS-RC-2 cells treated with a range of ouabain concentrations (0, 20, 40 and 80 nM) for 48 h, using a confocal microscope (magnification, x400). (G) Intracellular Ca^{2+} levels determined using a Fura-3/AM probe in NCI-H446 cells treated with a range of ouabain concentrations (0, 10, 20 and 40 nM) for 48 h, using a confocal microscope. (H) Intracellular ROS levels determined using a DCFH-DA probe in NCI-H446 cells treated with a range of ouabain concentrations (0, 10, 20 and 40 nM) for 48 h, using a confocal microscope. AO/EB, acridine orange/ethidium bromide; DCFH-DA, dichloro-dihydro-fluorescein diacetate; AM, acetoxymethylester; ROS, reactive oxygen species.

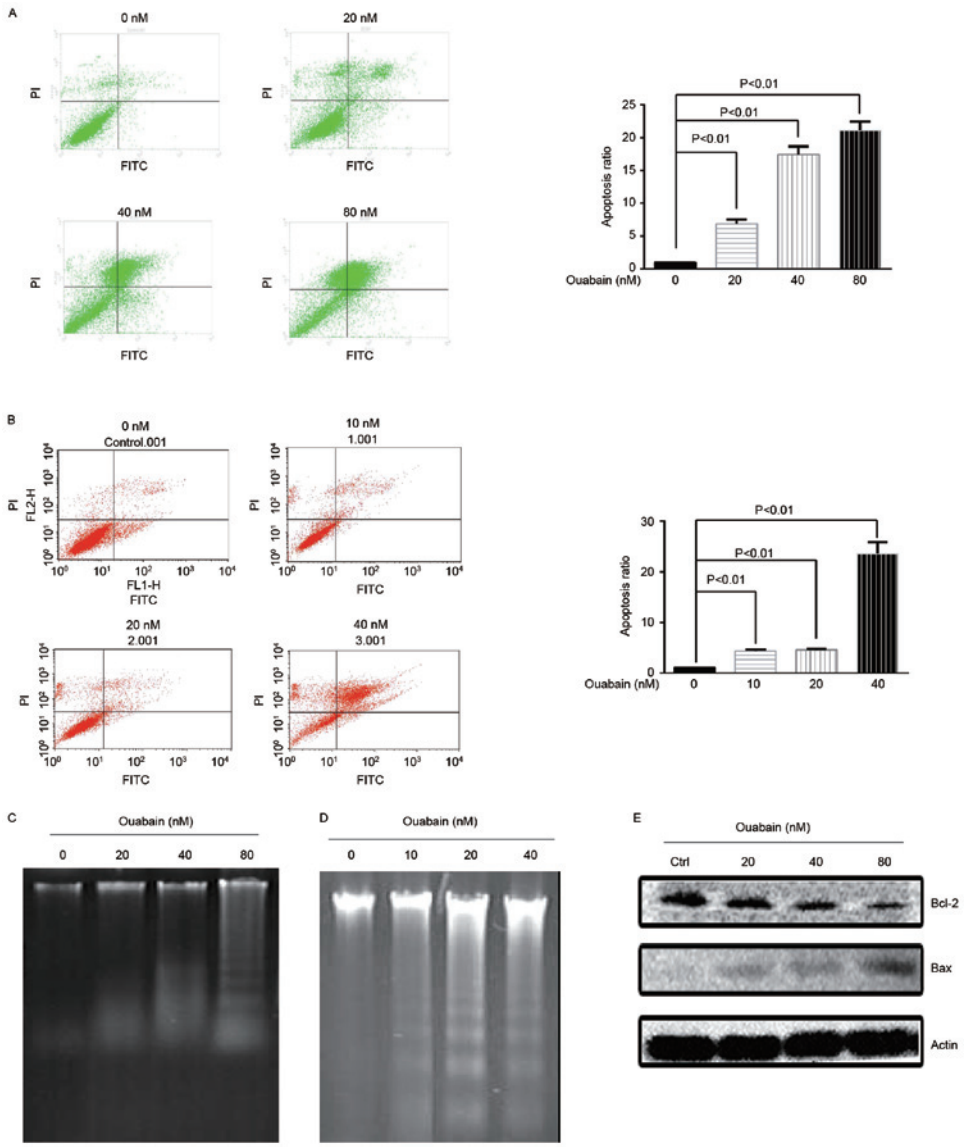

Figure 3. Ouabain induces apoptosis. (A) OS-RC-2 cells were treated with a range of ouabain concentrations (0, 20, 40 and 80 nM) for 48 h and flow cytometric analysis was performed to assess apoptosis using an AnnexinV-FITC/PI Apoptosis Detection kit. (B) NCI-H446 cells were treated with a range of ouabain concentrations (0, 10, 20 and 40 nM) for 48 h and flow cytometric analysis was performed to assess apoptosis using an AnnexinV-FITC/PI Apoptosis Detection kit. (C) OS-RC-2 cells were treated with a range of ouabain concentrations (0, 20, 40 and 80 nM) for 48 h and then DNA laddering was visualized following separation by gel electrophoresis. (D) NCI-H446 cells were treated with a range of ouabain concentrations (0, 10, 20 and 40 nM) for 48 h and then DNA laddering was visualized following separation by gel electrophoresis. (E) Bax and Bcl-2 protein expression was determined in OS-RC-2 cells treated with a range of ouabain concentrations (0, 20, 40 and 80 nM) for 48 h, using western blotting. FITC, fluorescein isothiocyanate; PI, propidium iodide; Bcl-2, B-cell lymphoma 2; Bax, Bcl-2-associated X protein.

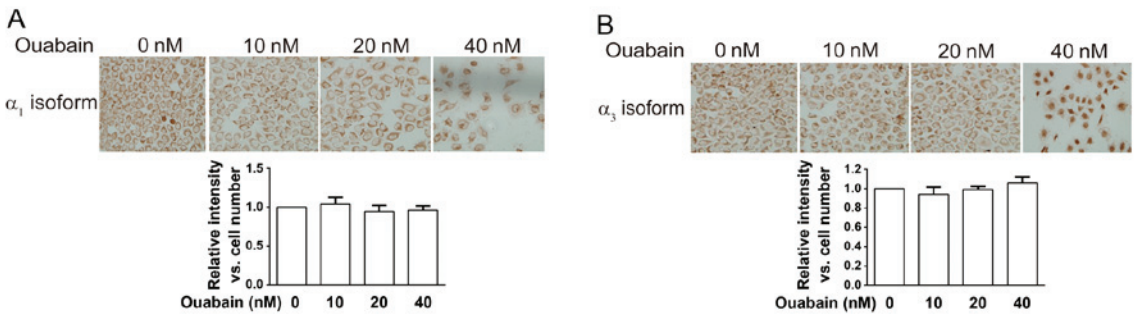

Figure 4. Ouabain does not affect the expression of the NKA α_1 and α_3 isoforms. NCI-H446 cells were treated with a range of ouabain concentrations (0, 10, 20 and 40 nM) for 48 h and immunocytochemistry staining was performed to determine the expression levels of (A) the NKA α_1 and (B) α_3 isoforms. NKA, Na^+/K^+-ATPase; ICC.

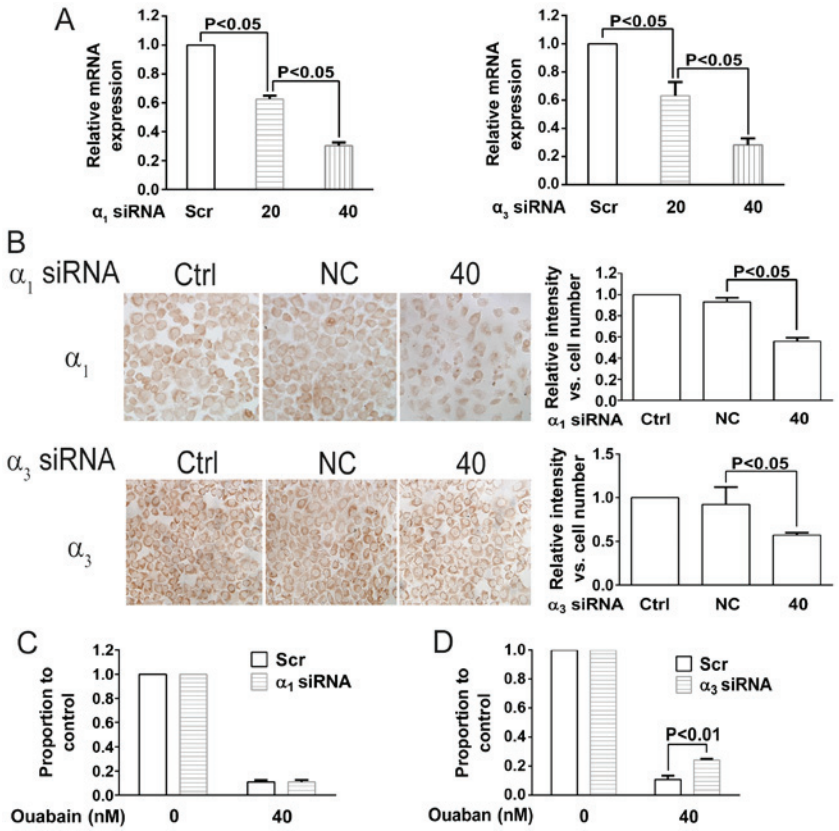

Figure 5. Cancer cell sensitivity to ouabain is associated with NKA isoform α_3 expression but not α_1. (A) NKA α_1 and α_3 isoformm RNA expression was determined in NCI-H446 cells transfected with siRNAs targeting each isoform and treated with 20 or 40 nM ouabain for 48 h using reverse transcription polymerase chain reaction. (B) NKA α_1 and α_3 isoform protein expression levels were determined in NCI-H446 cells transfected with siRNAs targeting each isoform and treated with 40 nM ouabain for 48 h using immunocytochemistry. NCI-H446 cells transfected with (C) α_1 siRNA or (D) α_3 siRNA were treated with 40 nM ouabain. Cell viability was determined using the MTT assay. NKA, Na^+/K^+-ATPase; siRNA, small interfering RNA; scr, scramble; ctrl, control; α_1 siRNA, siRNA targeting α_1 NKA isoform; α_3 siRNA, siRNA targeting α_3 NKA isoform; NC, negative control.

The clinical use of ouabain for the treatment of heart failure and atrial fibrillation is well established. Additionally, a number of studies have demonstrated that ouabain possesses antitumor activity (11,18-20). However, several concerns, including high cytotoxicity (20), remain to be addressed and little is known about the anticancer mechanism of ouabain.

The results of the present study demonstrated that NKA inhibition by ouabain inhibits cell proliferation and induces apoptosis, indicating that NKA serves a critical function in cell growth and survival. To examine the associations of NKA isoforms with ouabain sensitivity, siRNA-mediated knockdown of NKA α_1 and α_3 isoforms was performed. siRNAs targeting the NKA α_1 and α_3 isoforms downregulated the mRNA and protein expression of each isoform, respectively. However, only the NKA α_3 isoform siRNA partially rescued the cells from ouabain-induced growth inhibition, suggesting that the anticancer effect of ouabain may be associated with the NKA α_3 isoform. NKA α_3 isoform-knockdown did not fully reverse the growth inhibition, even though the effect was statistically significant; suggesting that other factors may be involved in the anticancer effect of ouabain. Further research is required to elucidate the underlying molecular mechanisms. The results of the present study demonstrated that NKA inhibition attenuates cellular proliferation and induces apoptosis, mediated by increased Ca^{2+} and ROS intracellular levels. NKA α_3 isoform siRNA knockdown impaired the antiproliferative effect of ouabain, suggesting that ouabain preferentially binds to the NKA α_3 isoform. These results indicated that the NKA α_3 isoform may be the anticancer molecular target of ouabain. Future research, should concentrate on further investigating the anticancer mechanism of ouabain and reducing its cardiotoxicity.

Acknowledgments

The present study was supported by the National Natural Science Foundation of China (grant no. 31640053), the Natural Science Foundation of Fujian Province (grant nos. 2016Y0029, 2016J01149 and 2016J01146) and the open Scientific Foundation of Fujian Key Laboratory (grant no. 2014ZDSY2002).

References

1. Jemal A, Bray F, Ferlay J, Ward E and Forman D: Global cancer statistics. CA Cancer J Clin 61: 69-90, 2011.
2. Jorgensen PL, Hakansson KO and Karlish SJ: Structure and Mechanism of Na, K-ATPase: Functional Sites and Their Interactions. Ann Rev Physiol 65: 817-849, 2003.
3. Baker Bechmann M, Rotoli D, Morales M, Maeso Mdel C, García Mdel P, Ávila J, Mobasheri A and Martín-Vasallo P: Na, K-ATPase isozymes in colorectal cancer and liver metastases. Front Physiol 7: 9, 2016.
4. Skou JC: The influence of some cations on an adenosine triphosphatase from peripheral nerves. Biochim Biophys Acta 23: 394-401, 1957.

5. Zhuang L, Xu L, Wang P, Jiang Y, Yong P, Zhang C, Zhang H, Meng Z and Yang P: Na^+/K^+ -ATPase α1 subunit, a novel therapeutic target for hepatocellular carcinoma. Oncotarget 6: 28183-28193, 2015.
6. Prassas I and Diamandis EP: Novel therapeutic applications of cardiac glycosides. Nat Rev Drug Discov 7: 926-935, 2008.
7. Kong D, Li J, Zhao B, Xia B, Zhang L, He Y, Wang X, Gao L, Wang Y, Jin X and Lou G: The effect of SCF and ouabain on small intestinal motility dysfunction induced by gastric cancer peritoneal metastasis. Clin Exp Metastasis 32: 267-277, 2015.
8. Shin HK, Ryu BJ, Choi SW, Kim SH and Lee K: Inactivation of Src-to-ezrin pathway: A possible mechanism in the ouabain-mediated inhibition of A549 cell migration. Biomed Res Int 2015: 537136, 2015.
9. Yan X, Liang F, Li D and Zheng J: Ouabain elicits human glioblastoma cells apoptosis by generating reactive oxygen species in ERK-p66SHC-dependent pathway. Mol Cell Biochem 398: 95-104, 2015.
10. Ninsontia C and Chanvorachote P: Ouabain mediates integrin switch in human lung cancer cells. Anticancer Res 34: 5495-5502, 2014.
11. Mijatovic T, Van Quaquebeke E, Delest B, Debeir O, Darro F and Kiss R: Cardiotonic steroids on the road to anti-cancer therapy. Biochim Biophys Acta 1776: 32-57, 2007.
12. Newman RA, Yang P, Pawlus AD and Block KI: Cardiac glycosides as novel cancer therapeutic agents. Mol Interv 8: 36-49, 2008.
13. Xu ZW, Wang FM, Gao MJ, Chen XY, Shan NN, Cheng SX, Mai X, Zala GH, Hu WL and Xu RC: Cardiotonic steroids attenuate ERK phosphorylation and generate cell cycle arrest to block human hepatoma cell growth. J Steroid Biochem Mol Biol 125: 181-191, 2011.
14. Livak KJ and Schmittgen TD: Analysis of relative gene expression data using real-time quantitative PCR and the 2(-Delta Delta C(T)) method. Methods 25: 402-408,2001.
15. Liu J, Tian J, Haas M, Shapiro JI, Askari A and Xie Z: Ouabain interaction with cardiac Na^+/K^+-ATPase initiates signal cascades independent of changes in intracellular Na^+ and Ca^{2+} concentrations. J Biol Chem 275: 27838-27844, 2000.
16. Majno G and Joris I: Apoptosis, oncosis, and necrosis: An overview of cell death. Am J Pathol 146: 3-15, 1995.
17. Hengartner MO: The biochemistry of apoptosis. Nature 407: 770-776, 2000.
18. Stenkvist B: Is digitalis a therapy for breast carcinoma? Oncol Rep 6: 493-499, 1999.
19. Haux J: Digitoxin is a potential anticancer agent for several types of cancer. Med Hypotheses 53: 543-548, 1999.
20. Winnicka K, Bielawski K and Bielawska A: Cardiac glycosides in cancer research and cancer therapy. Acta Pol Pharm 63: 109-115, 2006.